

## Article

# Facial Expressions Based Automatic Pain Assessment System

Thoria Alghamdi <sup>1,2,\*</sup> and Gita Alaghband <sup>1</sup>

<sup>1</sup> Department of Computer Science and Engineering, College of Engineering, University of Colorado Denver, Denver, CO 80204, USA; gita.alaghband@ucdenver.edu

<sup>2</sup> Department of Information Systems, College of Computing and Information Technology, King Abdulaziz University, Jeddah 21589, Saudi Arabia

\* Correspondence: thoria.alghamdi@ucdenver.edu

**Abstract:** Pain assessment is used to improve patients' treatment outcomes. Human observers may be influenced by personal factors, such as inexperience and medical organizations are facing a shortage of experts. In this study, we developed a facial expressions-based automatic pain assessment system (FEAPAS) to notify medical staff when a patient suffers pain by activating an alarm and recording the incident and pain level with the date and time. The model consists of two identical concurrent subsystems, each of which takes one of the two inputs of the model, i.e., "full face" and "the upper half of the same face". The subsystems extract the relevant input features via two pre-trained convolutional neural networks (CNNs), using either VGG16, InceptionV3, ResNet50, or ResNeXt50, while freezing all convolutional blocks and replacing the classifier layer with a shallow CNN. The concatenated outputs in this stage is then sent to the model's classifier. This approach mimics the human observer method and gives more importance to the upper part of the face, which is similar to the Prkachin and Soloman pain intensity (PSPI). Additionally, we further optimized our models by applying four optimizers (SGD/ADAM/RMSprop/RAdam) to each model and testing them on the UNBC-McMaster shoulder pain expression archive dataset to find the optimal combination, InceptionV3-SGD. The optimal model showed an accuracy of 99.10% on 10-fold cross-validation, thus outperforming the state-of-the-art model on the UNBC-McMaster database. It also scored 90.56% on unseen subject data. To speed up the system response time and reduce unnecessary alarms associated with temporary facial expressions, a select but effective subset of frames was inspected and classified. Two frame-selection criteria were reported. Classifying only two frames at the middle of 30-frame sequence was optimal, with an average reaction time of at most 6.49 s and the ability to avoid unnecessary alarms.

**Keywords:** computer vision; deep learning; inceptionv3; pain assessment; ResNet-50; ResNeXt50; transfer learning; VGG16



**Citation:** Alghamdi, T.; Alaghband, G. Facial Expressions Based Automatic Pain Assessment System. *Appl. Sci.* **2022**, *12*, 6423. <https://doi.org/10.3390/app12136423>

Academic Editors: Yang-Lang Chang, Mohammad Alkhaleefah and Tan-Hsu Tan

Received: 18 April 2022

Accepted: 21 June 2022

Published: 24 June 2022

**Publisher's Note:** MDPI stays neutral with regard to jurisdictional claims in published maps and institutional affiliations.



**Copyright:** © 2022 by the authors. Licensee MDPI, Basel, Switzerland. This article is an open access article distributed under the terms and conditions of the Creative Commons Attribution (CC BY) license (<https://creativecommons.org/licenses/by/4.0/>).

## 1. Introduction

Effective management of pain, including assessment and tracking overtime, is necessary to study the effectiveness of different treatments [1,2] and to avoid reaching chronic pain syndromes [2]. Pain can be assessed either by patients' self-reporting or by medical member observations [1,3]. The self-report method on a verbal or visual scale is the gold standard of pain assessment [1,4], but this method can be inaccurate and challenging in people with severely impaired communication ability (e.g., people with later stage dementia [5], burn-injured adults [1], neonates [6], intensive care patients [7], etc.). There are two common methods for pain assessment based on the observation principle: the Critical Care Pain Observation Tool (CPOT) and the Pain Assessment in Advanced Dementia Scale (PAINAD) [1]. The CPOT and PAINAD tools are designed for patients unable to self-report [1]. The CPOT assesses facial expressions, body movements, ventilator compliance, and muscle tension/rigidity, while the PAINAD assesses breathing, vocalization, facial expressions, body language, and consolability [1]. Facial expressions form the basic

components of pain assessment in both the CPOT and PAINAD tools. Studies have shown that periodically monitoring patient pain level in intensive care units in hospitals improved patient outcomes [8]. However, the medical member observations methods are highly subjective; human observers may be influenced by personal factors [6] and observers need to have the required experience [9]. Further, contentious pain assessment monitoring may fail and not be sustained when there is a shortage of medical experts [9]. These causes show the need for an automatic system to monitor a patient's pain level [6,8,9], which can also be used at home for elderly people [9]. A previous study that compared the performance of a human observer's pain assessment with that of an automated pain assessment from facial expressions concluded that the latter outperforms the former and is more reliable [6]. However, the tasks of pain detection and assessment from the images is challenging due to the diversity in head poses and environments, such as the illumination conditions and intensive occlusion [8,9]. Furthermore, patients tend to show a high variance in their reactions and facial expressions to the same level of pain [8].

The actions that form the facial expression of feelings, such as lowering the eyebrows or squinting, are called action units (*AU*) and each is assigned a unique code (e.g., *AU6* is lifting the cheeks). Regarding pain expression, six *AU*'s (*AU4*, 6, 7, 9, 10, and 43) have been found to be the most representative [10]. By assigning numerical values to those six *AUs*, pain can be calculated via the Prkachin and Soloman pain intensity (*PSPI*) equation, as shown below:

$$PSPI\ pain = AU4 + \max(AU6, AU7) + \max(AU9, AU10) + AU43 \quad (1)$$

This *PSPI* score determines pain intensity on a scale of 0 (no pain) to 16 (maximum pain). Below is a detailed explanation of the valuation of the six *AUs* used in *PSPI*:

- *AU4* is the intensity of lowering the eyebrows on a scale from 0 to 5 (0 = not lowered, 5 = maximally lowered).
- *AU6* is the intensity of raising the cheeks on a scale from 0 to 5 (0 = not raised, 5 = maximally raised).
- *AU7* is the intensity of tightening the eyelid on a scale from 0 to 5 (0 = not tight, 5 = very tight).
- *AU9* is the intensity of wrinkling the nose on a scale from 0 to 5 (0 = not wrinkled, 5 = very wrinkled).
- *AU10* is the intensity of rising the upper lip on a scale from 0 to 5 (0 = not raised, 5 = very raised).
- *AU43* is whether the eyes are closed; represented as a binary value (0 = opened, 1 = closed)

In this paper, we developed a new facial-expression-based automatic pain assessment system (FEAPAS). The model uses a dual convolutional neural network classifier to detect pain from facial expressions. The dual model better imitates the human brain's visual perception [11]. In this new model, we used the upper partition of detected faces, namely the eyes/brow area, and the full face as input images for our dual classifier. Because our goal was to produce an online model with a fast response time to generate alerts in a timely manner, we avoided an extensive computation time typically needed for deep learning system by using the optimal one of four pretrained networks (VGG16, InceptionV3, ResNet50, ResNeXt50) after freezing all the convolutional blocks and using the resulting weight in our shallow dual CNN classifier (e.g., transfer learning).

Using a camera, the proposed FEAPAS monitors a patient in bed; the backend code reads the video frame by frame and sends each frame to the classifier after detecting the patient's face and extracting the upper face area. An alarm is activated if the classifier outputs a positive pain score. The specific frame is stored with the associated pain level, date, and time to include in the report for the medical team.

To achieve a fast and robust FEAPAS, the following two challenges must be overcome. First, the system's performance heavily depends on the classifier's performance; a classifier

with high accuracy and a fast prediction process increases the system's reliability. To obtain an efficient classifier and overcome the limited face shapes in the system training dataset, transfer-learning is used on four CNN models (VGG16, InceptionV3, ResNet50, ResNeXt50) via freezing convolutional layers and replacing the prediction layer with a shallow CNN. This is then tested with four different optimizers (SGD, ADAM, RMSprop, and RAdam). The following two critical measurements were considered when developing the optimal concurrent shallow CNN with VGG16/InceptionV3/ResNet50/ResNeXt50 with frozen layers, i.e., the accuracy of 10-fold cross-validation and the accuracy of test data for an unseen subject. The resulting shallow model was embedded in our FEAPAS to generate timely and accurate alerts.

The second challenge is to speed up the system's response time. To do so, we selectively sampled the frames being tested. Instead of testing every single frame in the input sequence, we tested two frame-selection approaches. The first approach tests two segments from each end of a video sequence (boundary test), while the second tests one segment in the middle of the video sequence frames (middle test).

The rest of the paper is organized as follows: Section 2 reviews transfer learning models and optimizers; Section 3 includes previous research on automatic pain assessment in chronological order; Section 4 describes the dataset and the proposed models; Section 5 presents the experimental results; and Section 6 offers concluding remarks.

## 2. Background

The transfer learning method is used to speed up training process and improve the performance of new untrained models by using the weights of an existing model [12]. The concept of transfer learning is modeled after human intelligence by using the current knowledge to solve new problems faster or better [13]. In transfer learning, the top layers of a pretrained model are frozen and specific layers above it are added to create a new model [12]. However, the benefit of transfer learning is affected by the data and task of the new model [13]. We chose to test the four VGG16, InceptionV3, ResNet50, and ResNeXt50 as possible platforms for classifier for FEAPAS because they have been widely successful in image classification.

In the ILSVRC 2014 competition, Visual Geometry Group VGG16 was ranked the best method in localization and second best in classification [12]. VGG16 addressed the depth of CNN architecture by adding more layers with small filters ( $3 \times 3$ ). VGG16 was trained on ImageNet with 1000 classes. The structure of VGG16 is shown in Figure 1 [14].

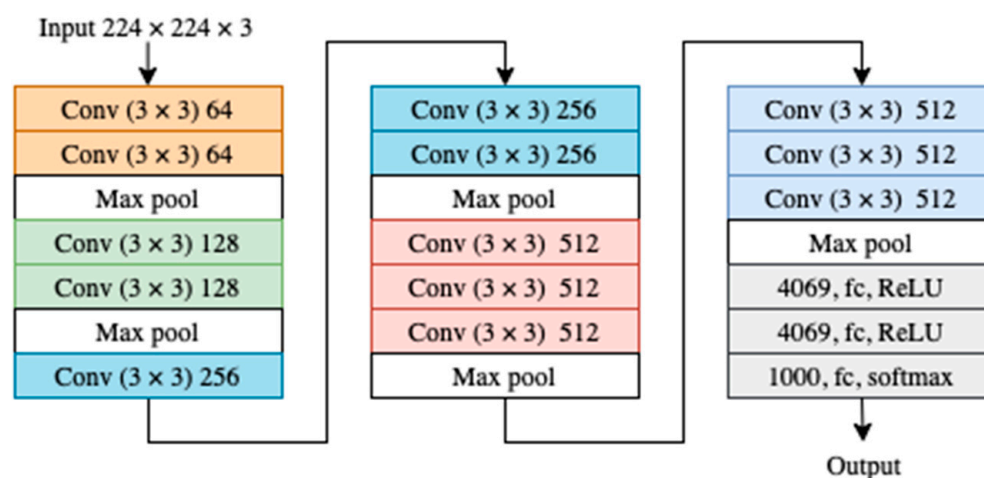


**Figure 1.** VGG16 architecture where each color represents a block of layers with the same kernel size.

InceptionV1 won the ILSVRC 2014 classification. It was proposed to overcome the overfitting of the data in the deep convolutional neural networks by using multiple filters of different sizes on the same level [15]. InceptionV3 is designed to optimize the performance

of the previous versions of inception which suffer from high computations by applying factorized convolutions and aggressive regularization [16].

The residual neural network (ResNet) won ILSVRC 2015 in image classification, detection, and localization. Moreover, it won MS COCO 2015 detection and segmentation. ResNet was inspired by VGG even though it is deeper and less complex [17].

Neural networks may become less efficient as the number of layers increase and the model deepens [18–20]. ResNet adds a direct connection to the layers of the network to solve the problem of vanishing gradients, which arises from the deep depth of the network. This connection preserves a certain percentage of the output of the previous network layers [18–20]. Deep neural networks have more layers where wide neural networks have more kernels. However, a study comparing wider and deeper neural networks showed that shallow networks outperformed the much deeper residual networks in classification and segmentation [20]. In fact, the number of trainable parameters is the cause of ResNet performance [20]. The structure of ResNet50 is shown in Figure 2 [17].

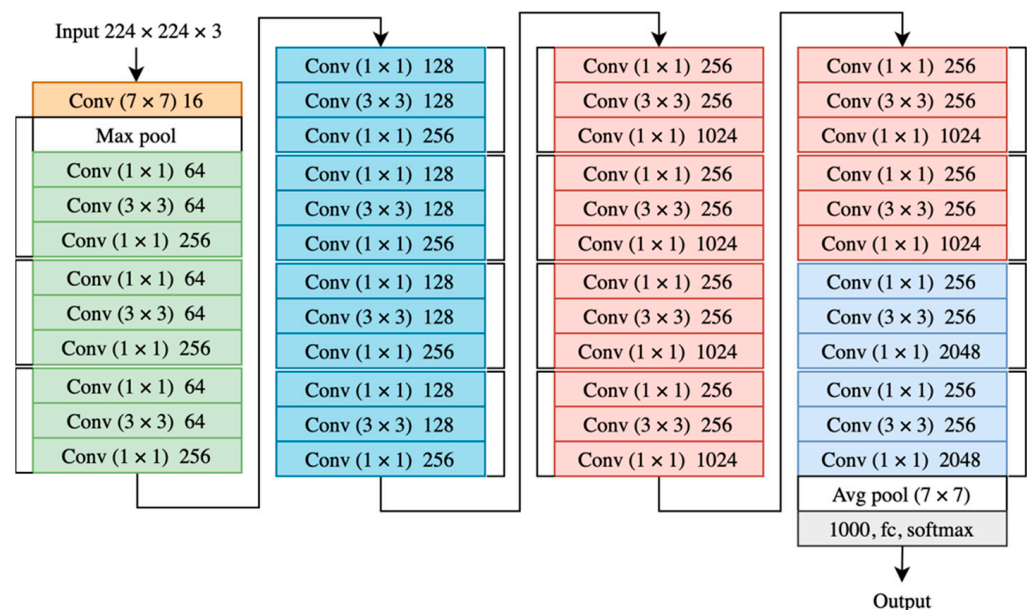


**Figure 2.** ResNet50 architecture where each color represents a block of layers with the same kernel size.

ResNeXt was a runner up in ILSVRC 2015. It was designed to overcome the complexity in ResNet, which emerge from staking the modules of the same topology. ResNeXt inspired its structure from the inception model and used a simpler branch design method than inception [21,22].

The optimizer algorithm plays a critical role in the neural network training process. Studies have investigated the performance and declared a specific optimizer to work better with a particular problem [23–25].

The stochastic gradient descent (SGD) is the popular algorithm for solving optimization problems, but it requires manually adjusting the learning rate decay [23,24]. To overcome this manual process in SGD, Diederik P. Kingma proposed adaptive moment estimation (ADAM). ADAM makes the model converge faster and occupies little memory [24,25]. Root mean square propagation RMSProp is an optimization algorithm first proposed by Geoffrey E. Hinton to speed up the model convergence through loss function optimization [24]. Where ADAM and RMSProp suffer from the variance in adaptive learning rate, rectified ADAM (RAdam) has effectively solved it [26,27].

### 3. Related Work

The early studies in the field of pain assessment extracted the features from frames using the active appearance model (AAM) and used a support vector machine (SVM) clas-

sifier [28,29] to create automated pain assessment systems. Khan et al. [30] later compared SVM in their proposed framework for pain along with three other classifiers (decision tree (DT), random forest (RF), and 2 nearest neighbors (2NN) based on Euclidean distance). Their framework detects the face from a frame, horizontally halves the detected face, and uses the halves as the two inputs of the model; it employs the shape information using a pyramid histogram of oriented gradients (PHOG) and the appearance information using a pyramid local binary pattern (PLBP) to obtain a unique representation of the face. However, more recent pain assessments utilize neural networks. Zhou et al. [31] utilized the recurrent convolutional neural network (RCNN) to introduce a real-time regression framework for automatic pain intensity estimation, while Rodriguez et al. [32] employed the advantage of combining CNNs with long short-term memory (LSTM) in their model. Some researchers even used dual models that consisted of a fusion structure of CNNs, such as Semwal and Londhe, who used two shallow neural networks—spatial appearance network (SANET) and shape descriptor network (SDNET)—in one model [9], and multiple neural networks in another [33].

Inspired by Khan et al. [30], our proposed model used two inputs based on the detected face parts to mimic the PSPI code; however, instead of using both halves of the face we used the full face as one input and the upper face for the other input. We employed neural networks for automatic feature extraction from frames, just as [31] and [32] did. However, instead of RCNN or a combination of CNNs and LSTM, we employed the VGG16, InceptionV3, ResNet50, and ResNeXt50 each with a shallow CNN replacing the classifier layer.

The higher accuracy obtained by [9] and [33] encouraged us to adopt a fusion structure of CNNs.

We compared our model's performance to the aforementioned models [9,30,32,33] that used the same dataset (UNBC-McMaster shoulder pain expression archive), as well as the measurement strategy (the k-fold cross validation accuracy), as ours. Vaish and Sagar's state-of-the-art model [34], which employed Kaze algorithm to extract features from the detected face, obtains a fisher vector and sends it to an SVM classifier. It also uses the same testing dataset and metric measurements. Therefore, we compared our results against it. The resulting optimal model is then embedded in our FEAPAS system.

## 4. Methodology

### 4.1. Dataset

In this study, we used a subset of the UNBC-McMaster shoulder pain expression archive dataset [10]. To develop an automatic pain assessment system based on facial expressions, researchers at McMaster University and the University of Northern British Columbia recorded 200 sequences for 25 adult participants (12 males and 13 females) suffering from shoulder pain. The recording sessions were conducted while the participants were performing a series of active and passive physical tests on their affected and unaffected limbs. The UNBC-McMaster shoulder pain expression archive dataset consists of 200 sequences with a total of 48,398 colored frames of  $320 \times 240$  pixels.

The UNBC-McMaster shoulder pain expression archive dataset is highly imbalanced; 82.71% represents the "no pain" class with 40,029 images and only 17.29% represents the different levels of pain with 8369 images. Thus, using the full dataset may result in a biased classification, as shown in [9,33]. To avoid such potential bias, we used a subset with 6000 randomly selected frames of 24 participants. We classified the subset dataset into four classes: no pain, low pain, moderate pain, and severe pain. Each had 1500 frames. The no pain class included images with PSPI equals zero. The low pain class included images with PSPI equals 1. The moderate pain class included images with a PSPI equal to 2. The severe pain class included images with a PSPI equal to or greater than 3. Table 1 shows details of our subset data.

**Table 1.** Our subset data description.

| The Class | Label         | PISP Code | Number of Images |
|-----------|---------------|-----------|------------------|
| 1         | No Pain       | 0         | 1500             |
| 2         | Low Pain      | 1         | 1500             |
| 3         | Moderate Pain | 2         | 1500             |
| 4         | Severe Pain   | 3+        | 1500             |

The no pain class represents the normal situation, whereas the low pain, moderate pain, and severe pain classes represent attention-drawing situations. Thus, the alarm should be activated for these three classes. Additionally, 80% of the subset data was used for training and 20% was used for validation. Figure 3 shows samples of the UNBC-McMaster shoulder pain expression archive dataset.



**Figure 3.** Samples of the UNBC-McMaster shoulder pain expression archive dataset with different levels of pain. Reprinted/adapted with permission from Ref. [10]. Copyright (@jeffery Cohn).

To test the data, we used all frames that belonged to the unseen participant. They were coded as “064-ak064” and totaled 1611 frames.

To validate the FEAPAS, the consecutive frames in the unseen testing sequences were merged using OpenCV library to create 6 test videos (one for each sequence) with 4 frames per second each. Table 2 shows details of each video.

**Table 2.** Testing videos description.

| The Video | Label      | Number of Merged Frames | Duration in Second |
|-----------|------------|-------------------------|--------------------|
| Video 1   | Sever pain | 397                     | 99                 |
| Video 2   | Sever pain | 308                     | 77                 |
| Video 3   | Sever pain | 337                     | 84                 |
| Video 4   | No pain    | 142                     | 35                 |
| Video 5   | Sever pain | 263                     | 65                 |
| Video 6   | No pain    | 165                     | 41                 |

#### 4.2. Data Preprocessing

Face detection is a critical process in pain assessment models. In [30,34], researchers used the Viola Jones object detection algorithm [35] to detect the face before feeding the data to the model. In [3,33], researchers used the multi-task cascades neural network (MTCNN) [36] for face localization purposes as a milestone step in preparing the data. Due to good results of MTCNN in detecting faces, especially when compared against Haar Cascades, we used MTCNN for face detection and removed unnecessary information in each image. The next step was to divide the detected face into two parts: an upper part, which contained the eyes and eyebrows, and a lower part, which contained the nose, mouth, and chin [30]. We used OpenCV for this task. Unlike in a previous study [30], where the upper and lower parts of the detected face were used as inputs to the model, we used the upper face and the full face as inputs to simulate the PSPI code as a way to focus more on the eyes and brows than the lower face.

To measure the impact of illumination and head rotation in our model performance, we used the OpenCV library to vary the brightness and rotation of the testing data of unseen subject.

#### 4.3. The Model

This study was conducted in two phases. First, we developed a robust classifier to detect when a person was in pain. Second, we developed an efficient system capable of detecting when a person was in pain, generating an alarm while minimizing false alarms.

##### 4.3.1. Classifier

The UNBC-McMaster shoulder pain expression archive dataset, which we used to train our system, resulted from experiments conducted on 25 participants, providing little face-shape variation. To overcome the limitations of face shape variety and to combat overfitting due to data scarcity, we used ImageNet weights to initialize our models before fine-tuning our custom dataset. This approach yielded better results than training each model from scratch on the domain dataset. Our model extracted features from the detected face and the upper part of the detected face of our subset dataset using VGG16 in the first experiment, InceptionV3 in the second experiment, ResNet50 in the third experiment, and ResNeXt50 in the fourth experiment after freezing the convolutional blocks and dropping the final prediction layers. Transfer learning processes in VGG16 and ResNet50 were conducted by extracting the feature vectors and freezing all convolutional blocks, as well as feeding the output to our new classifier (Figure 4).

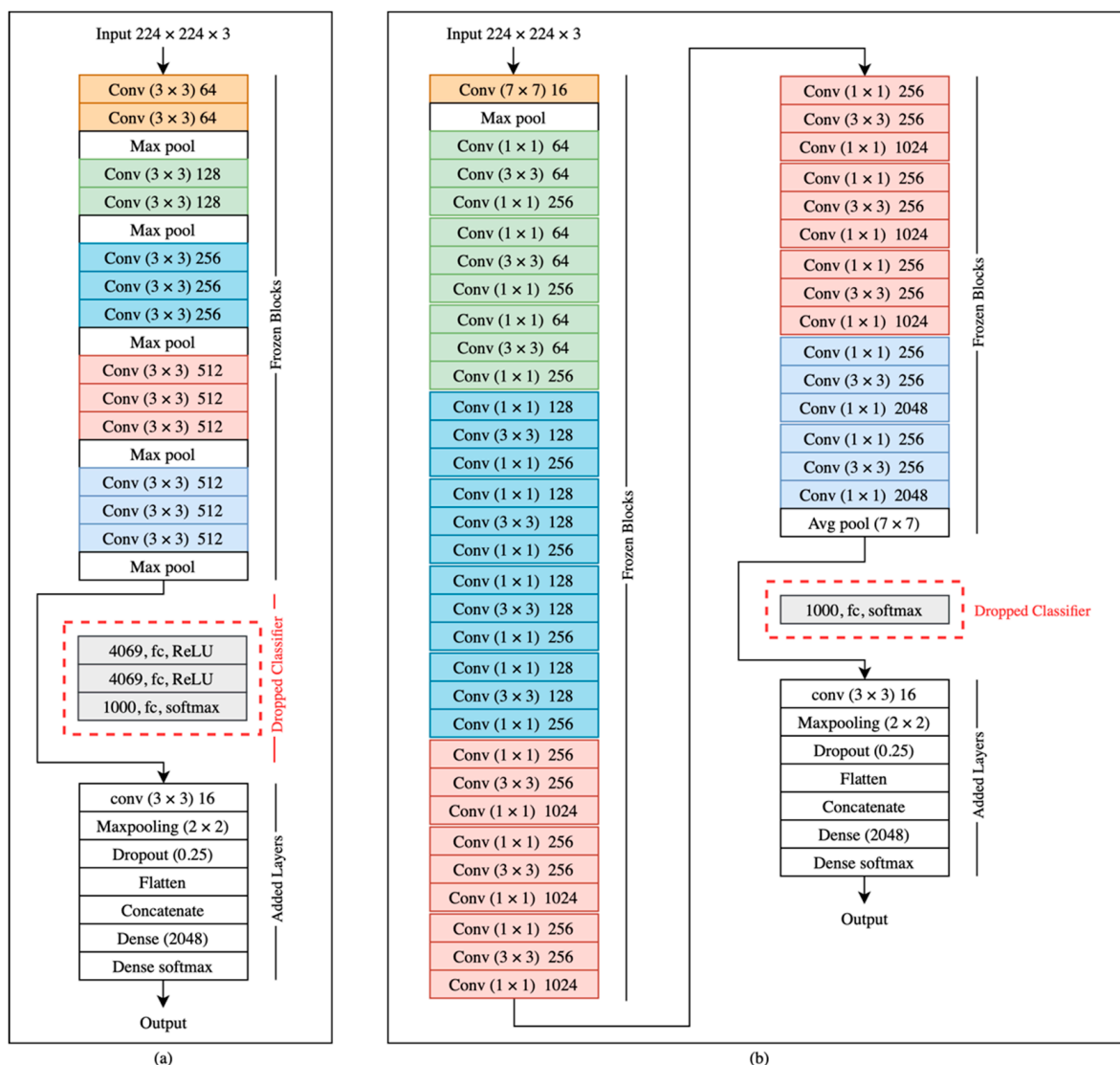


**Figure 4.** The transfer learning using (a) VGG16 and (b) ResNet50.

Using VGG16, ResNet50, or ResNeXt50 alone did not meet the desired accuracy. We used them to extract the relevant features and replaced their prediction layers with a 4-layer concurrent shallow CNN to increase the model accuracy. The features were extracted from two inputs: the lower face and the upper face. They were sent to two identical shallow CNNs, each consisting of four layers (Figure 5). The first layer was convolution (Conv2D), which contained 16 neurons, a  $(3 \times 3)$  filter, and Relu activation function. The second layer was the max-pooling layer, which had a  $(2 \times 2)$  filter. The third layer was the dropout with a probability of 0.25. The fourth layer was a flattened layer. The output of each branch of CNN was concatenated and sent to a dense layer with 2048 neurons, then to a fully connected layer to classify the data. The shallow CNNs parameters above were chosen after extensive experiments with different values. The InceptionV3 model is shown in Figure 6. The models were trained with four optimizers (i.e., SGD-ADAM-RSMprop-RAdam). The differentiation between these 16 models was based on the higher accuracy of 10-fold cross-validation and testing data of the unseen subject. The best model was subjected to a few more tests to measure its performance under different brightness and rotations. These brightness/rotations tests were conducted on the modified testing data, as described in Section 4.2.



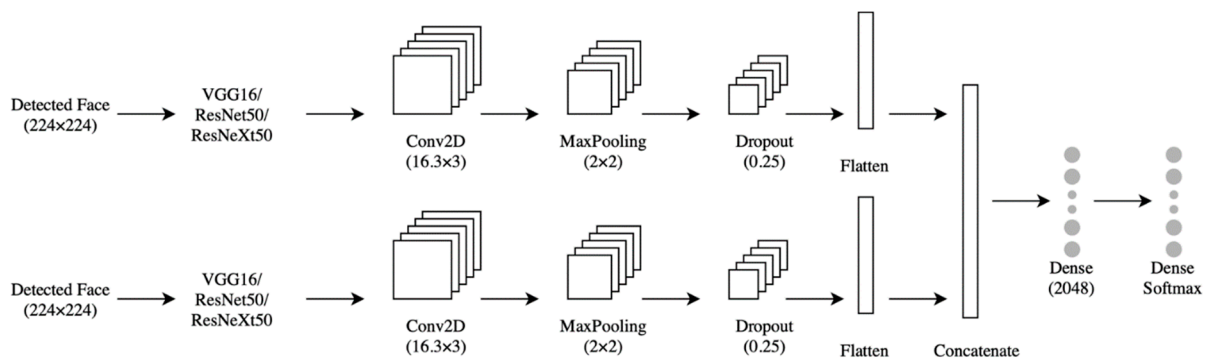


Figure 5. The concurrent shallow CNN model using (VGG16/ResNet50/ResNeXt50) with frozen layers.

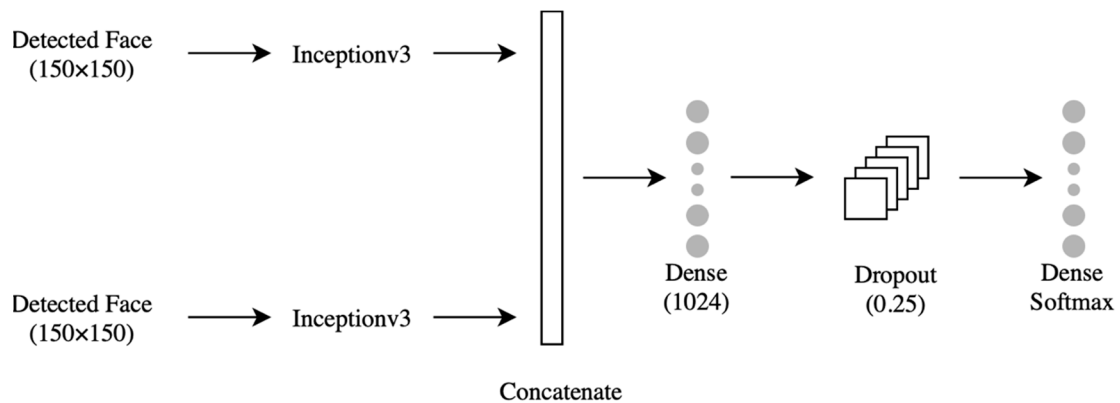


Figure 6. The concurrent shallow CNN model using InceptionV3 with frozen layers.

#### 4.3.2. Facial Expression-Based Automatic Pain Assessment System FEAPAS

To avoid unnecessary alarms arising from temporary potential situations, such as the blinking of the eyes, FEAPAS does not classify every frame in a video sequence. While we tested various combinations, we herein report our results on testing two frame-selection approaches. The first approach (the boundary test) tested two segments at the two ends of a sequence of frames. The second approach (the middle test) tested one segment at the middle of a sequence of frames. Figure 7a,b illustrate the two approaches, where  $N$  is the length of the sequence (in the number of frames). Let  $2\Delta$  be the total number of frames being tested. Then, for the boundary test, the first and last  $\Delta$  frames are classified. For the middle test,  $2\Delta$  frames centered around the middle of the sequence ( $N/2$ ) are classified.

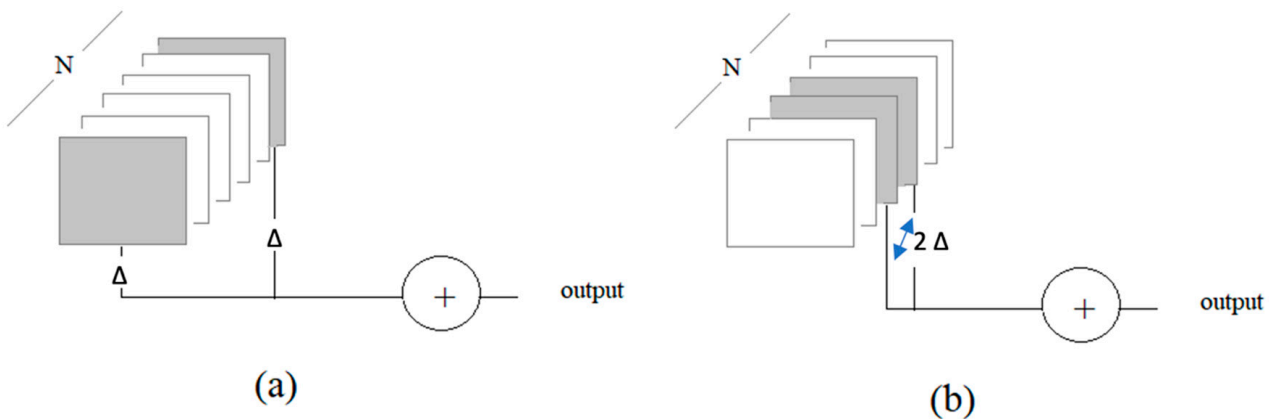


Figure 7. Frame selection approaches: (a) boundary test and (b) middle test.

The automatic pain assessment system reads the online video frame-by-frame and selects  $2\Delta$  frames out of every  $N$  video sequence block based on the frame-selection ap-

proach. The selected frames are then processed to obtain the inputs of the InceptionV3-SGD classifier, which is the upper- and full-face partitions. If the classifier’s output is not set to no pain for all tested frames in the N-frame sequence, then the alarm is activated. Figure 8 shows a high-level flow chart of the automatic pain assessment system, FEAPAS. In the boundary testing frame-selection method, the final decision is taken after classifying the last frame in the sequence, but, in the middle testing approach, the decision is immediately released after reading half the number of frames in the sequence, which speeds up the response time.

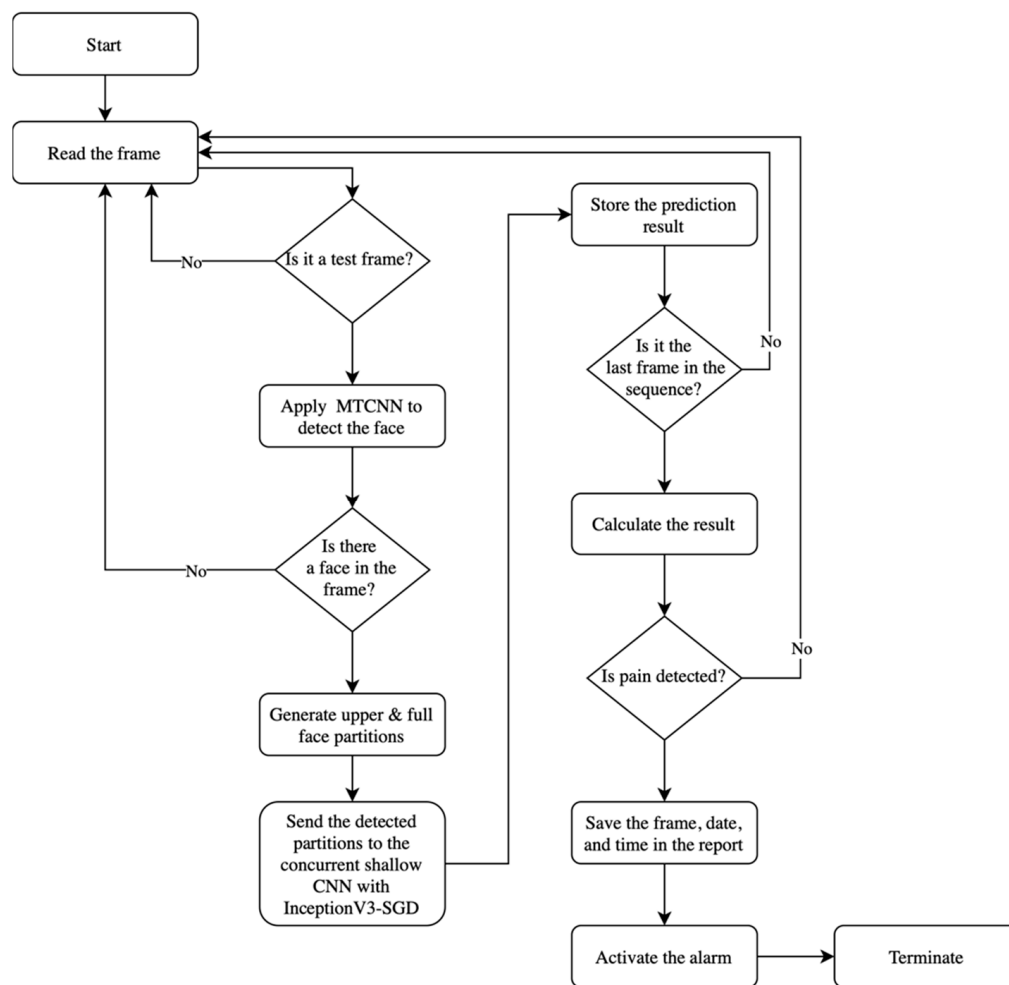


Figure 8. FEAPAS flow chart.

We used Anaconda on a GPU Tesla P100-SXM2 [37] to build and train the models. To test the selection frame approaches on FEAPAS, we used a CPU Intel Core i7-8750 (2.20GHz and 8 GB RAM), with a Windows 10 64-bit operating system (Anaconda 5.3.1.) [38]; Library Keras 2.2.4. [39]; Library OpenCV 4.4.0. [40]; and programming language Python 3.7.3.

### 5. Results

Table 3 shows the 10-fold cross validation results of the 16 models (precision, recall, and F1-score). Table 4 shows the results of the phase that tested the two classifier platforms in terms of the 10-fold cross validation accuracy and data of unseen subject for 16 assortments made up of four models and four optimizers trained on the UNBC-McMaster shoulder pain expression archive dataset. All 16 models showed high accuracy and achieved more than 96.00% for 10-fold cross validation, except for ResNeXt50 with SGD. For an unseen subject, InceptionV3 with SGD and ResNeXt50 with SGD achieved 90.56% and 90.19, respectively, whereas ResNet50 with ADAM and InceptionV3 with RAdam achieved 88.21% and 86.10%,

respectively. The rest of the models achieved less than 85.00%. As shown in Figure 9, the SGD optimizer was more stable and less fluctuating in InceptionV3 training comparing with other optimizers (i.e., ADAM, RMSprop, and RAdam).

**Table 3.** The 10-fold cross validation results of VGG16, InceptionV3, ResNet50, and ResNeXt50 with four optimizers.

| The Model   | The Optimizer | Precision | Recall | F1-Score |
|-------------|---------------|-----------|--------|----------|
| VGG16       | SGD           | 98.42     | 98.58  | 98.47    |
|             | ADAM          | 99.84     | 99.81  | 99.83    |
|             | RMSprop       | 99.12     | 99.17  | 99.14    |
|             | RAdam         | 99.30     | 99.84  | 99.81    |
| InceptionV3 | SGD           | 99.84     | 99.81  | 99.83    |
|             | ADAM          | 97.33     | 96.94  | 97.05    |
|             | RMSprop       | 99.94     | 99.93  | 99.96    |
|             | RAdam         | 99.51     | 99.48  | 99.49    |
| ResNet50    | SGD           | 99.84     | 99.81  | 99.83    |
|             | ADAM          | 99.84     | 99.81  | 99.83    |
|             | RMSprop       | 99.84     | 99.81  | 99.83    |
|             | RAdam         | 99.84     | 99.81  | 99.83    |
| ResNeXt50   | SGD           | 96.99     | 96.89  | 96.90    |
|             | ADAM          | 99.68     | 99.65  | 99.67    |
|             | RMSprop       | 99.84     | 99.81  | 99.83    |
|             | RAdam         | 99.69     | 99.63  | 99.66    |

**Table 4.** Results of VGG16, InceptionV3, ResNet50, and ResNeXt50 with four optimizers.

| The Model   | The Optimizer | 10-Fold Cross Validation Accuracy (%) | Accuracy of Unseen Person (%) | Average Accuracy (%) |
|-------------|---------------|---------------------------------------|-------------------------------|----------------------|
| VGG16       | SGD           | 97.41                                 | 82.06                         | 89.74                |
| VGG16       | ADAM          | 99.12                                 | 78.15                         | 88.64                |
| VGG16       | RMSprop       | 97.90                                 | 66.05                         | 81.98                |
| VGG16       | RAdam         | 99.30                                 | 65.80                         | 82.55                |
| InceptionV3 | SGD           | 99.10                                 | 90.56                         | <b>94.83</b>         |
| InceptionV3 | ADAM          | 97.45                                 | 84.48                         | 90.97                |
| InceptionV3 | RMSprop       | 98.27                                 | 82.37                         | 90.32                |
| InceptionV3 | RAdam         | 96.93                                 | 86.10                         | 91.52                |
| ResNet50    | SGD           | 96.58                                 | 76.10                         | 86.34                |
| ResNet50    | ADAM          | 99.23                                 | 88.21                         | 93.72                |
| ResNet50    | RMSprop       | 99.28                                 | 83.86                         | 91.57                |
| ResNet50    | RAdam         | 99.27                                 | 83.61                         | 91.44                |
| ResNeXt50   | SGD           | 89.85                                 | 90.19                         | 90.02                |
| ResNeXt50   | ADAM          | 97.98                                 | 74.98                         | 86.48                |
| ResNeXt50   | RMSprop       | 98.18                                 | 71.14                         | 84.96                |
| ResNeXt50   | RAdam         | 98.40                                 | 80.76                         | 89.58                |

Bold number shows the best result.

Analyzing the results of the trained models helped us decide which deep-learning framework worked better with our FEAPAS system. Based on the combination of the two accuracy values, InceptionV3 with SGD was selected as the models to be inserted in the FEAPAS system. We therefore conducted more experiments on the FEAPAS system to evaluate the overall performance.

Table 5 shows that our proposed approach outperformed previous approaches that were also conducted on the same UNBC-McMaster shoulder pain expression archive dataset and evaluated based on k-fold cross validation. The accuracy of the unseen subject was not provided by previous publications, so we could not compare. Table 5 also shows whether the study used entire images in the dataset, a subset, or a variation of subset plus data collected from other sources.

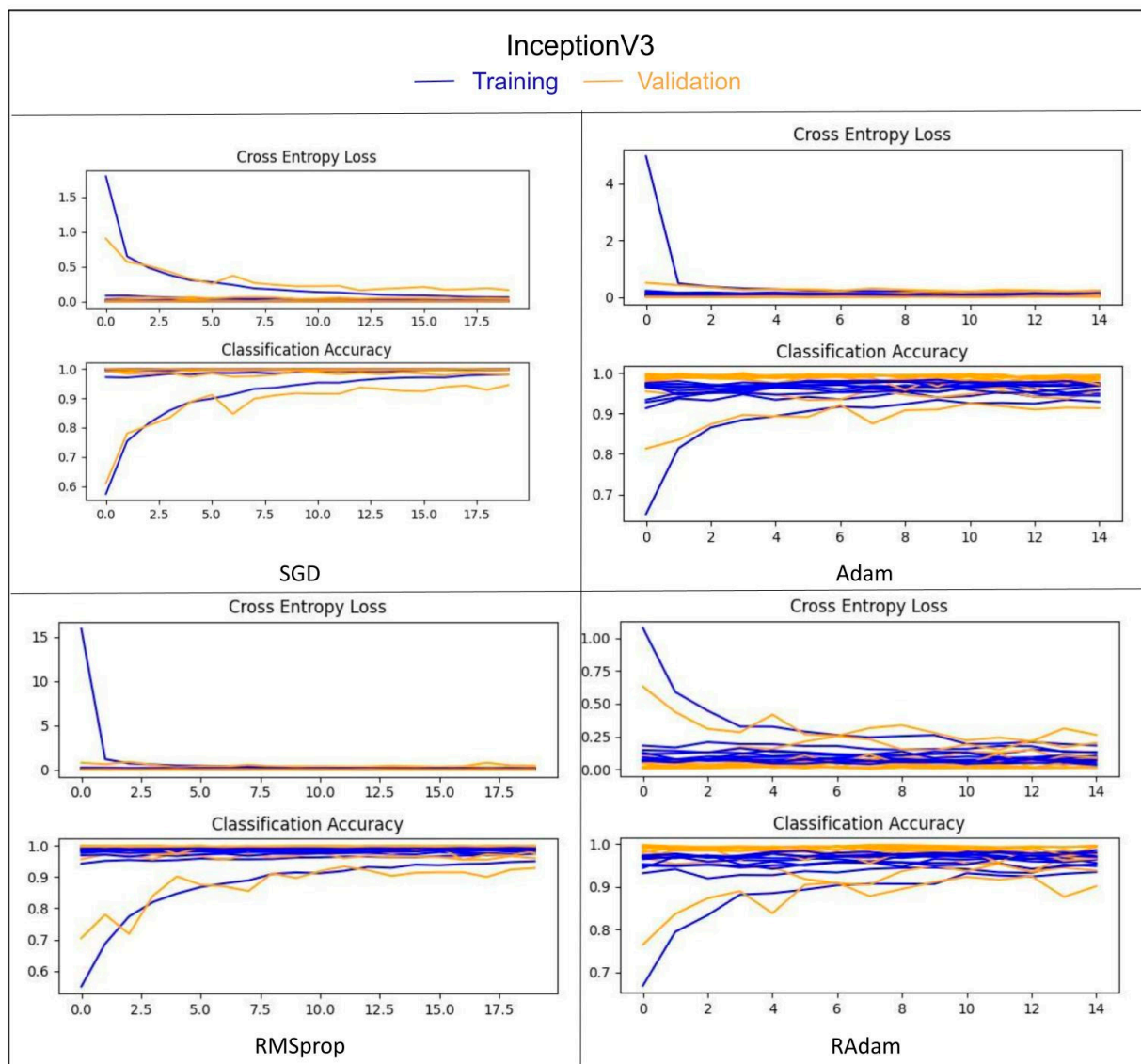


Figure 9. The convergence curves in InceptionV3 training with four optimizers.

Table 5. Comparison with other approaches using UNBC-McMaster dataset.

| Approach                 | Use All Images in Dataset  | Number of Used Images                                      | Number of Classes                     | k-Fold Cross Validation Accuracy (%) | Accuracy of Unseen Subject (%) |
|--------------------------|--|--|---------------------------------------|--------------------------------------|--------------------------------|
| Khan et al. [30]         | Yes  | 40,029 No pain<br>8369 Pain                                | 2                                     | 96.40                                |                                |
| P. Rodriguez et al. [32] | No   | -  | 2                                     | 83.00                                |                                |
| Semwal and Londhe [9]    | No   | 16,000   | 4 [0,1,(2 + 3),(4 + 5 <sup>+</sup> )] | 94.00                                |                                |
| Semwal and Londhe [33]   | No + collected data of 10 patients suffering from pain in a clinic | 16,000 from UNBC-McMaster + 16,460 from the collected data | 4                                     | 96.00                                |                                |
| Vaish and Sagar [34]     | No   | -  | 4                                     | 91.87                                |                                |
| Proposed approach        | No   | 6000   | 4 [0,1,2,3 <sup>+</sup> ]             | 99.10                                | 90.65                          |

To measure the impact of brightness and head rotation on the InceptionV3 with SGD model, we applied the model on the three adjusted testing data (unseen subject) and recorded the accuracy for each testing data. Table 6 shows the impact of illumination and head rotation of the dataset on the InceptionV3 with SGD model’s accuracy, as compared to its 90.65% accuracy on the original testing data. As Table 5 shows, increasing the brightness dropped the accuracy by 00.81% while decreasing the brightness and the head rotation had no negative effect on the efficiency of the model.

**Table 6.** The impact of brightness and head rotation on the InceptionV3\_SGD model.

| Dataset                            | Accuracy (%) | Performance (%) |
|------------------------------------|--------------|-----------------|
| The brightened images              | 89.75        | −00.81          |
| The dimmed images                  | 91.56        | +00.91          |
| The images with a slight rotation. | 91.17        | +00.52          |

To test the response time of our system, we ran FEAPAS four times, i.e., twice for each frame selection approach using sequence length values ( $N = 30$ ).

The experiment was conducted by playing the test videos on a screen and directing the laptop's webcam to the screen to mimic a real live feed. A stopwatch was used to record the time, at which point the alarm was activated.

We tested the following four scenarios with a sequence length of  $N = 30$ . The middle and boundary frame selection strategies with a segment length of  $2\Delta$  are as follows:

- One frame at each end of the sequence: two-boundary test frames: 2-B,  $\Delta = 1$
- Two frames at the middle of the sequence: two-middle test frames: 2-M,  $\Delta = 1$
- Two frames at each end of the sequence: four-boundary test frames: 4-B,  $\Delta = 2$
- Four frames at the middle of the sequence: four-middle test frames: 4-M,  $\Delta = 2$

Table 7 shows the impact of frame selection approach in response time. The larger segment length required more frames to be classified, which thus led to longer response time. Finishing classification at the middle or at the end of the sequence was an important factor and should be considered in future studies. Moreover, 2-M-30 showed the lowest average response time of 6.49 s, and 4-B-30 showed the highest average response time of 29.86 s.

**Table 7.** The response time in seconds for four running, where B denotes boundary testing and M denotes middle testing. Further, [2–4] is the number of testing frames and [30] is the length of sequence. For example, 4-B-30 indicated that the FEAPAS tested four frames on the boundary of the sequence with 30 frames for each decision. If all four frames are classified as pain, then FEAPAS activates the alarm and stores the tested frames/images with date, time, and pain level.

|             | 2-B-30   | 2-M-30   | 4-B-30   | 4-M-30   |
|-------------|----------|----------|----------|----------|
| Video 1     | 32.97    | 12.34    | 40.38    | 15.93    |
| Video 2     | 03.33    | 02.95    | 06.70    | 12.45    |
| Video 3     | 07.05    | 06.09    | 07.76    | 06.11    |
| Video 4     | No alarm | No alarm | No alarm | No alarm |
| Video 5     | 48.31    | 06.89    | 51.96    | 07.11    |
| Video 6     | No alarm | No alarm | No alarm | No alarm |
| The average | 27.68    | 6.49     | 29.86    | 6.61     |

Figure 10 shows the output of FEAPAS on video 1 by using the 2-B-30 selected frame strategy. The FEAPAS stored the captured frames and classified them as pain before saving the date and time with the pain level.



('16:27:01 on Friday, June the 10th, 2022', array([3], dtype=int64), array([2], dtype=int64))

**Figure 10.** The output of FEAPAS on video 1 using the 2-B-30 strategy. Reprinted/adapted with permission from Ref. [10]. Copyright (@jeffery Cohn).

## 6. Conclusions

We developed a new facial expression-based automatic pain assessment system to monitor patients and assist in the pain evaluation process. The FEAPAS was designed to recognize four classes: no pain, low pain, moderate pain, and severe pain. When a patient is detected to be in pain, FEAPAS activates an alarm to allow the medical team to take steps. While developing FEAPAS, we focused on two main criteria: (1) the system should be precise enough to not miss any true alarm and (2) fast enough to catch the pain situations and activate the alarm. Our proposed FEAPAS consisted of two subsystems each using a modified pretrained CNN. The modification included freezing the convolutional block and replacing the prediction layer with a shallow CNN. Each subsystem takes one of the two systems' inputs (i.e., the full face and the upper face). Among the 16 tested model combinations (four pretrained CNN options, VGG16, InceptionV3, ResNet50, and ResNeXt50, and four possible optimizers, SGD, ADAM, RMSprop, and RAdam), the model with a InceptionV3 and the SGD optimizer excelled with an accuracy of 99.10% on 10-fold cross-validation, and a 90.56% score on the unseen subject data. (Future work should explore other optimizers to further improve system performance.) To speed up the response time in FEAPAS and avoid unnecessary alarms caused by momentary facial expressions, we classified few selected frames instead of classifying every single frame. Further, we tested, two frame selection approaches (i.e., at the two ends of the sequence and in the middle of the sequence) using sequence lengths of 30 frames with segment-lengths of two and four frames, respectively. FEAPAS correctly classified six online videos with 1611 frames (four videos recorded the severe pain situation and two other videos recorded the no pain situation) with an average response time of less than 30 s.

**Author Contributions:** T.A. conducted this research under supervision of her PhD advisor, G.A. The authors contributed toward the new methodologies, design, implementation, and analysis of FEAPAS application. All authors have read and agreed to the published version of the manuscript.

**Funding:** This research received no external funding.

**Institutional Review Board Statement:** Not applicable.

**Informed Consent Statement:** Permission to use the UNBC-McMaster shoulder pain expression dataset to develop an automatic pain assessment system based on facial expressions was received from the McMaster University and the University of Northern British Columbia. Permission is granted to use a specific set of images (TV095, JL047, IB109, DM039, AK064) for electronic media and include notice of copyright (@jeffery Cohn).

**Data Availability Statement:** Data was obtained from [10], and accessed on 9 November 2021, and are available [at <http://www.pitt.edu/~emotion/um-spread.htm>] with the permission of [10].

**Conflicts of Interest:** The authors declare no conflict of interest.

## References

1. Taggart, S.; Skylas, K.; Brannelly, A.; Fairbrother, G.; Knapp, M.; Gullick, J. Using a Clinical Judgement Model to Understand the Impact of Validated Pain Assessment Tools for Burn Clinicians and Adult Patients in the ICU: A Multi-Methods Study. *Burns* **2021**, *47*, 110–126. [[CrossRef](#)]
2. Laloo, C.; Kumbhare, D.; Stinson, J.N.; Henry, J.L. Pain-QuILT: Clinical Feasibility of a Web-Based Visual Pain Assessment Tool in Adults with Chronic Pain. *J. Med. Internet Res.* **2014**, *16*, e3292. [[CrossRef](#)]
3. Semwal, A.; Londhe, N.D. ECCNet: An Ensemble of Compact Convolution Neural Network for Pain Severity Assessment from Face Images. In Proceedings of the 2021 11th International Conference on Cloud Computing, Data Science & Engineering (Confluence), Noida, India, 28–29 January 2021. [[CrossRef](#)]
4. Lints-Martindale, A.; Hadjistavropoulos, T.; Lix, L.M.; Thorpe, L. A Comparative Investigation of Observational Pain Assessment Tools for Older Adults with Dementia. *Clin. J. Pain* **2012**, *28*, 226–237. [[CrossRef](#)]
5. Natavio, T.; McQuillen, E.; Dietrich, M.S.; Wells, N.; Rhoten, B.A.; Vallerand, A.H.; Monroe, T.B. A Comparison of the Pain Assessment Checklist for Seniors with Limited Ability to Communicate (PACSLAC) and Pain Assessment in Advanced Dementia Scale (PAINAD). *Pain Manag. Nurs.* **2020**, *21*, 502–509. [[CrossRef](#)]
6. Salekin, S.; Zamzmi, G.; Goldgof, D.; Kasturi, R.; Ho, T.; Sun, Y. Multimodal Spatio-Temporal Deep Learning Approach for Neonatal Postoperative Pain Assessment. *Comput. Biol. Med.* **2021**, *129*, 104150. [[CrossRef](#)]

7. Othman, E.; Werner, P.; Saxen, F.; Al-Hamadi, A.; Gruss, S.; Walter, S. Automatic Vs. Human Recognition of Pain Intensity from Facial Expression on the X-ITE Pain Database. *Sensors* **2021**, *21*, 3273. [[CrossRef](#)]
8. Rudovic, O.; Pavlovic, V.; Pantic, M. Automatic Pain Intensity Estimation with Heteroscedastic Conditional Ordinal Random Fields. In *Advances in Visual Computing*; Springer: Berlin/Heidelberg, Germany, 2013.
9. Semwal, A.; Londhe, N.D. Computer aided pain detection and intensity estimation using compact CNN based fusion network. *Appl. Soft Comput.* **2021**, *112*, 107780. [[CrossRef](#)]
10. Lucey, P.; Cohn, J.F.; Prkachin, K.M.; Solomon, P.E.; Matthews, I. Painful data: The UNBC-McMaster shoulder pain expression archive database. In Proceedings of the 2011 IEEE International Conference on Automatic Face & Gesture Recognition (FG), Santa Barbara, CA, USA, 21–25 March 2011; pp. 57–64.
11. Yu, Y.; Hao, K.; Ding, Y. A New Image Classification Model Based on Brain Parallel Interaction Mechanism. *Neurocomputing* **2018**, *315*, 190–197. [[CrossRef](#)]
12. Dubey, A.K.; Jain, V. Automatic facial recognition using VGG16 based transfer learning model. *J. Inf. Optim. Sci.* **2020**, *41*, 1589–1596. [[CrossRef](#)]
13. Yang, Q. An introduction to transfer learning. In *Advanced Data Mining and Applications*; Tang, C., Ling, C.X., Zhou, X., Cercone, N.J., Li, X., Eds.; Lecture Notes in Computer Science; Springer: Berlin/Heidelberg, Germany, 2008; Volume 5139, p. 1.
14. Simonyan, K.; Zisserman, A. Very Deep Convolutional Networks for Large-Scale Image Recognition. *arXiv* **2014**, arXiv:1409.1556.
15. Szegedy, C.; Liu, W.; Jia, Y.; Sermanet, P.; Reed, S.; Anguelov, D.; Erhan, D.; Vanhoucke, V.; Rabinovich, A. Going Deeper with Convolutions. In Proceedings of the IEEE Conference on Computer Vision and Pattern Recognition (CVPR), Boston, MA, USA, 7–12 June 2014; pp. 1–9.
16. Szegedy, C.; Vanhoucke, V.; Ioffe, S.; Shlens, J.; Wojna, Z. Rethinking the Inception Architecture for Computer Vision. In Proceedings of the IEEE Conference on Computer Vision and Pattern Recognition (CVPR), Las Vegas, NV, USA, 27–30 June 2016; pp. 2818–2826. [[CrossRef](#)]
17. He, K.; Zhang, X.; Ren, S.; Sun, J. Deep Residual Learning for Image Recognition. In Proceedings of the 2016 IEEE Conference on Computer Vision and Pattern Recognition (CVPR), Las Vegas, NV, USA, 27–30 June 2016; pp. 770–778. [[CrossRef](#)]
18. Veit, A.; Wilber, M.J.; Belongie, S. Residual Networks Behave Like Ensembles of Relatively Shallow Networks. *arXiv* **2016**, arXiv:1605.06431v2.
19. Zagoruyko, S.; Komodakis, N. Wide Residual Networks. *arXiv* **2016**, arXiv:1605.07146.
20. Wu, Z.; Shen, C.; Van Den Hengel, A. Wider or Deeper: Revisiting the ResNet Model for Visual Recognition. *Pattern Recognit.* **2019**, *90*, 119–133. [[CrossRef](#)]
21. Xie, S.; Girshick, R.; Dollár, P.; Tu, Z.; He, K. Aggregated Residual Transformations for Deep Neural Networks. In Proceedings of the IEEE Conference on Computer Vision and Pattern Recognition (CVPR), Honolulu, HI, USA, 21–26 July 2016; pp. 5987–5995.
22. Li, L.; Ma, H. RDCTrans U-Net: A Hybrid Variable Architecture for Liver CT Image Segmentation. *Sensors* **2022**, *22*, 2452. [[CrossRef](#)] [[PubMed](#)]
23. Landro, N.; Gallo, I.; La Grassa, R. Mixing ADAM and SGD: A Combined Optimization Method. *arXiv* **2020**, arXiv:2011.08042.
24. Jiang, X.; Hu, B.; Satapathy, S.C.; Wang, S.-H.; Zhang, Y.-D. Fingerspelling Identification for Chinese Sign Language via AlexNet-Based Transfer Learning and Adam Optimizer. *Sci. Program.* **2020**, *2020*, 3291426. [[CrossRef](#)]
25. Jiang, S.; Chen, Y. Hand Gesture Recognition by Using 3DCNN and LSTM with Adam Optimizer. In *Advances in Multimedia Information Processing—PCM 2017*; Zeng, B., Huang, Q., El Saddik, A., Li, H., Jiang, S., Fan, X., Eds.; PCM 2017. Lecture Notes in Computer Science; Springer: Cham, Switzerland, 2018; Volume 10735. [[CrossRef](#)]
26. Liu, L.; Jiang, H.; He, P.; Chen, W.; Liu, X.; Gao, J.; Han, J. On the Variance of the Adaptive Learning Rate and Beyond. *arXiv* **2019**, arXiv:1908.03265.
27. Cui, K.; Zhan, Z.; Pan, C. Applying Radam Method to Improve Treatment of Convolutional Neural Network on Banknote Identification. In Proceedings of the 2020 International Conference on Computer Engineering and Application (ICCEA), Guangzhou, China, 18–20 March 2020. [[CrossRef](#)]
28. Ashraf, A.B.; Lucey, S.; Cohn, J.F.; Chen, T.; Ambadar, Z.; Prkachin, K.; Solomon, P.; Theobald, B.J. The Painful Face: Pain Expression Recognition using Active Appearance Models. In Proceedings of the 9th International Conference on Multimodal Interfaces, ACM, Nagoya, Aichi, Japan, 12–15 November 2007; pp. 9–14. [[CrossRef](#)]
29. Lucey, P.; Cohn, J.F.; Prkachin, K.M.; Solomon, P.E.; Chew, S.; Matthews, I. Painful Monitoring: Automatic Pain Monitoring using the UNBC-McMaster Shoulder Pain Expression Archive Database. *Image Vis. Comput.* **2012**, *30*, 197–205. [[CrossRef](#)]
30. Khan, R.A.; Meyer, A.; Konik, H.; Bouakaz, S. Pain Detection through Shape and Appearance Features. In Proceedings of the 2013 IEEE International Conference on Multimedia and Expo (ICME), San Jose, CA, USA, 15–19 July 2013. [[CrossRef](#)]
31. Zhou, J.; Hong, X.; Su, F.; Zhao, G. Recurrent Convolutional Neural Network Regression for Continuous Pain Intensity Estimation in Video. In Proceedings of the IEEE Conference on Computer Vision and Pattern Recognition (CVPR) Workshops, Las Vegas, NV, USA, 27–30 June 2016; pp. 84–92.
32. Rodriguez, P.; Cucurull, G.; Gonzalez, J.; Gonfaus, J.M.; Nasrollahi, K.; Moeslund, T.B.; Roca, F.X. Deep Pain: Exploiting Long Short-Term Memory Networks for Facial Expression Classification. *IEEE Trans. Cybern.* **2017**, *52*, 3314–3324. [[CrossRef](#)]
33. Semwal, A.; Londhe, N.D. MVFNet: A multi-view fusion network for pain intensity assessment in unconstrained environment. *Biomed. Signal Processing Control.* **2021**, *67*, 102537. Available online: <https://www.sciencedirect.com/science/article/pii/S1746809421001348> (accessed on 10 March 2022). [[CrossRef](#)]

34. Vaish, A.; Gupta, S. A Novel Approach for Pain Intensity Detection by KAZE Features. In *Proceedings of the Third International Conference on Microelectronics, Computing and Communication Systems*; Springer: Singapore, 2019.
35. Viola, P.; Jones, M. Rapid Object Detection using a Boosted Cascade of Simple Features. In *Proceedings of the 2001 IEEE Computer Society Conference on Computer Vision and Pattern Recognition*. CVPR 2001, Kauai, HI, USA, 8–14 December 2001; Volume 1. [[CrossRef](#)]
36. Zhang, K.; Zhang, Z.; Li, Z.; Qiao, Y. Joint Face Detection and Alignment using Multitask Cascaded Convolutional Networks. *IEEE Signal Processing Lett.* **2016**, *23*, 1499–1503. [[CrossRef](#)]
37. Parallel Distributed Systems Lab—PDS Lab. Available online: <http://pds.ucdenver.edu/> (accessed on 8 April 2022).
38. Anaconda | The World's Most Popular Data Science Platform. Available online: <https://www.anaconda.com> (accessed on 8 April 2022).
39. Keras. The Python Deep Learning API. Available online: <https://keras.io/> (accessed on 8 April 2022).
40. OpenCV 4.4.0—OpenCV. Available online: <https://opencv.org/opencv-4-4-0/> (accessed on 8 April 2022).